

Experimental evidence of a $1/H$ activation law in nanostructures with perpendicular magnetic anisotropy

J. Moritz,* B. Dieny, and J. P. Nozières

SPINTEC, URA CEA/CNRS, CEA/Grenoble, Avenue des Martyrs, 38054 Grenoble Cedex, France

Y. Pennec, J. Camarero, and S. Pizzini

Laboratoire Louis Néel, Polygone scientifique CNRS, Avenue des Martyrs, Boîte Postale 166, 38042 Grenoble Cedex, France.

(Received 22 December 2004; published 9 March 2005)

The dynamical reversal of the magnetization in perpendicular magnetized nanostructures with typical lateral sizes of about 100 nm has been studied by magneto-optical Kerr effect on time scales extending from the quasistatic regime down to 20 ns. By modeling the reversal dynamics using a thermally activated nucleation process, it has been shown that the barrier height depends on the inverse of the applied field. A clear saturation of the dynamical coercive force at a value close to the anisotropy field was observed in the nanosecond range. This study allows a new interpretation of magnetization reversal in perpendicular systems and leads to criteria of stability in magnetic recording media.

DOI: 10.1103/PhysRevB.71.100402

PACS number(s): 75.70.Kw, 75.60.Ch, 75.50.Vv

Controlling the magnetization reversal in thin magnetic layers is one of the fundamental issues in magnetic data storage. Since the data transfer rate in hard disk drives approaches the GHz range, the reversal of an individual bit should be achieved in the nanosecond time scale or even less. Over the last decade, several studies have addressed the magnetization reversal dynamics in storage media using tools based on microsquid,¹ magneto-optical Kerr effect² (MOKE) or magnetoresistance effects.³ In the sub-nanosecond time scale, these studies have focused on the precessional reversal of magnetization subject to a pulsed field.

At longer time scales and for nanoparticles, it has been shown that the reversal follows the Néel-Brown activation law and that the barrier height dependence on the field was of the Stoner-Wohlfarth (SW) form.¹ This last assumption applies when the particle size is below the domain wall width δ_B , a necessary condition to observe a coherent rotation of the spins. In the SW model and in some other theoretical developments,^{4,5} the barrier height ΔE follows a power law with the applied field H . The value of its exponent α is between $3/2$ and 2 depending on the orientation of the field with respect to the easy axis, and is written as

$$\Delta E = K_{eff} \left(1 - \frac{H}{H_K}\right)^2, \quad (1)$$

where K_{eff} is the effective anisotropy, V the volume of the particle, and H_K the anisotropy field.

In infinite magnetic layers, the reversal takes place through nucleation and domain wall propagation. In the propagation process, the energy barrier is associated with the depinning of the domain wall from the pinning centers.⁶ The nucleation process is usually described as a coherent reversal of the magnetization inside an activation volume (with an activation length larger than δ_B) with a barrier height chosen as for the SW model

$$\Delta E = E_n \left(1 - \frac{H}{H_n}\right)^\alpha, \quad (2)$$

where E_n and H_n are the nucleation energy and nucleation field, respectively. This approach is often known as the Sharrock model, which is widely used in interpreting the dynamic coercivity of recording media.^{7,8} Unfortunately, many dynamical measurements on thin layers, which present large magnetic aftereffects, cannot be explained with this model. As a matter of fact, the SW formulation is based on a balance between the Zeeman and anisotropy energies, both depending on the angle between the magnetization and the easy axis (in a simple uniaxial case). Despite the clear evidence of domain wall formation in the nucleation process, the exchange energy is not taken into account in this model. A way to introduce its effect on the reversal dynamics is to use the so-called droplet theory, where the free energy is expressed by a balance between volume and surface energy terms. Starting from Barbara's approach,⁹ an analytical formulation of the barrier height for the nucleation event can be obtained. The free energy for a cylindrical droplet of reversed magnetization in a perpendicular magnetized system is

$$E(r) = 2\pi r t \gamma - 2\pi \mu_0 r^2 t H M_S, \quad (3)$$

where r is the radius of the cylinder, t the thickness of the magnetic layer, M_S the magnetization, and γ the surface (or domain wall) energy, which is proportional to the square root of the product between the exchange A and the effective anisotropy constant K_{eff} . If the size of the nucleus is below the critical radius r_C given by $\partial_r E(r_C) = 0$, the droplet collapses. Above r_C , the nucleus is able to expand by domain wall propagation. The free energy for a cylindrical nucleus with a critical radius r_C is

$$E(r_C) = \frac{\pi t \gamma^2}{2\mu_0 H M_S}. \quad (4)$$

It is well known that nucleation takes place on local defects where A or K_{eff} are reduced due to impurities, dislocations, or grain boundaries. As a result, the surface tension γ is minimal on the defect and increases in the surrounding area. Considering that the highest gradient of γ is at a distance r_0 of the nucleation center, it is possible to define a critical field associated with this slope by

$$H_0 = \frac{1}{2\mu_0 M_S} \frac{\partial \gamma}{\partial r} \Big|_{r_{max}}. \quad (5)$$

The barrier height for reversal becomes $\Delta E = E(r_0, H_0) - E(r, H)$. When the wall energy depends on position, the droplet radius is related to the field by

$$r = \frac{1}{2\mu_0 H M_S} \frac{\partial(\gamma r)}{\partial r}. \quad (6)$$

Replacing the value of r and r_0 in the expression of the free energy (3), it becomes

$$\Delta E = 2\pi t(r_0 \gamma_0 - r\gamma) - \pi t \left[r_0 \left(\frac{\partial(r\gamma)}{\partial r} \right)_{r_0} - r \left(\frac{\partial(r\gamma)}{\partial r} \right) \right]. \quad (7)$$

Expression (7) is a Taylor development of the energy with respect to r , which can be rewritten as

$$\Delta E = 2\pi t(r_0 - r) \left[\left(\frac{\partial(r\gamma)}{\partial r} \right)_{r_0} - \pi \frac{d}{dr} \left(r \frac{\partial(r\gamma)}{\partial r} \right)_{r_0} \right] \quad (8)$$

At first order, the energy barrier is proportional to the difference $r - r_0$, which leads to the simple expression

$$\Delta E = \frac{\pi t \gamma^2}{2\mu_0 M_S} \left[\frac{1}{H} - \frac{1}{H_0} \right]. \quad (9)$$

Aharoni and Baltensperger have numerically calculated the total magnetic energy in the case of cylindrical and spherical nucleation centers in a bulk ferromagnet.¹⁰ For cylindrical centers, their numerical calculations have shown that the dependence of the energy on the applied field is close to the one obtained by the droplet model when the external field is small with respect to the anisotropy field. The agreement is even better for a spherical nucleus. In the droplet model, the problem is treated by calculating the barrier height between the initial and the final magnetic configuration neglecting the way the magnetization rotates inside the nucleus. This may lead to a difference in energy between the phenomenological and micromagnetic approaches.

Though the applied field reduces the barrier height when its amplitude increases, favoring one orientation of the magnetization, it is not the only effect acting on the reversal. The temperature also activates the overcoming of the energy barrier and its effect on the reversal time follows an Arrhenius law

$$\tau = \tau_0 \exp \left[\frac{\Delta E}{k_B T} \right], \quad (10)$$

where k_B is the Boltzmann constant, T the absolute temperature, and τ_0 an attempt reversal time. The calculation of τ_0

was carried out by Néel and Brown^{11,12} in the case of ferromagnetic systems. In this paper, τ_0 is kept constant (1 ns).

Under a constant negative applied field, the magnetization decreases exponentially from its positive saturated state to the negative one. This description of magnetic aftereffects can be adapted to the case where the field varies with a constant sweep rate. Each branch of the hysteresis loop is a succession of aftereffect experiments where the time taken by the magnetization to relax to the equilibrium is governed by the field sweep rate. The differential equation describing the time evolution of the magnetization M can be expressed as

$$\int_{M_s}^M \frac{dM}{M + M_s} = \int_0^H - \frac{dH}{\tau \frac{dH}{dt}}. \quad (11)$$

In this last expression, the initial configuration of the magnetization is chosen saturated along the easy axis, i.e., perpendicular to the film plane. The external field is applied in the opposite direction. dH/dt denotes the applied field sweep rate and will be called v in the rest of this paper. Using the barrier form (9), it is easy to calculate the form of the M vs H hysteresis branch

$$\frac{M(H)}{M_s} = 2 \exp \left(- \frac{1}{\tau_0 v} \exp \frac{\Lambda}{H_0} \right) \times \exp \left[H \exp \frac{-\Lambda}{H} - \Lambda \Gamma \left(0, \frac{\Lambda}{H} \right) \right] - 1, \quad (12)$$

with $\Lambda = (\pi t \gamma^2) / (2M_S k_B T)$ and Γ defined as $\Gamma[a, z] = \int_z^\infty t^{a-1} e^{-t} dt$.

The thermal activation effects as well as the field dependence of the barrier height can be evaluated by magnetic aftereffect or temperature experiments. In this paper, we carried out dynamic coercivity measurements on patterned and unpatterned Pt/Co films exhibiting a strong perpendicular-to-plane anisotropy. The patterning has been performed by electron-beam lithography and etching techniques onto Si wafers. The size of the structures varied between 100×100 and 100×400 nm² with an edge-to-edge spacing constant of about 100 nm. The deposition of the multilayered structures following the nanostructuring of the Si was performed by magnetron sputtering. In previous studies, we have shown that each dot is exchange decoupled from its neighbors even if the magnetic layer covers the top of the dots, their sides, and the trenches between them.¹³ The dependence of the coercive field on the applied field sweep rate was measured using the MOKE setup. Hysteresis loops were acquired with field sweep rates v from 1 to 10 MT/s corresponding to reversal times ranging from 1 s to 20 ns. The external field was generated using a ferrite electromagnet below 2 kT/s and with microcoils in the fastest dynamical regime. The current through these micromachined coils was produced by a voltage discharge through a capacitors bank.¹⁴

As the magnetic signal measured by MOKE is integrated on the laser beam area, the hysteresis loops represent, for the patterned layers, the contributions of a large number of dots (the spot-size radius was about 500 μ m). Figure 1 shows

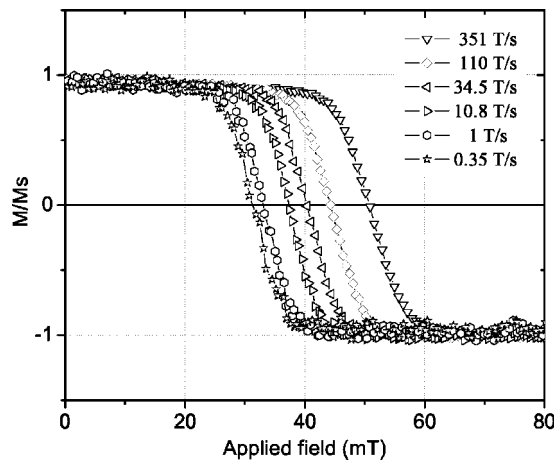


FIG. 1. Right branches of hysteresis loops measured by polar Kerr effect for several applied field sweep rates onto an array of magnetic $100 \times 100 \text{ nm}^2$ dots. The spot size was of about $500 \mu\text{m}$ of diameter.

several hysteresis loops for an array of $100 \times 100 \text{ nm}^2$ dots and for different v . By measuring the average coercive field of the array, we can determine the variation of the dynamical coercivity of the average particle.¹⁵ This evolution is plotted on Fig. 2(a) and compared with the case of the unpatterned layer on Fig. 2(b). At first sight, the general shape of both variations looks quite similar although the increase in the coercive field in the investigated range of field sweep rate (from 1 mT/s to 2 kT/s) is quite different (of the order of 15 for the unpatterned layer and of 3 for the dots). This is explained by a different magnetization reversal in both structures. In the continuous layer, the reversal is mostly achieved by the propagation of domain walls after the nucleation barriers are overcome. At low frequencies, only a few nucleation centers are sufficient to provoke the complete reversal. When v increases, the nucleation rate increases

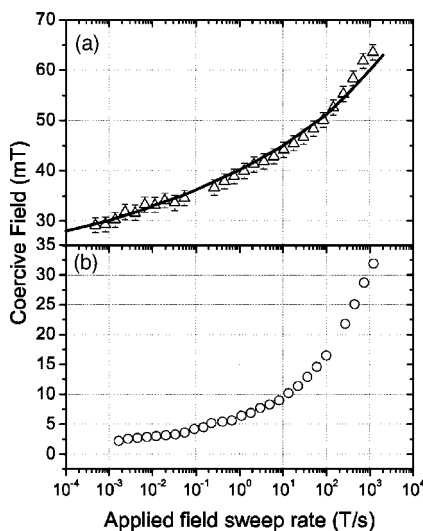


FIG. 2. Evolution of the average dynamical coercive field vs the field sweep rate for the magnetic dots (a) and for the unpatterned layer (b). The continuous line on (a) is a fit using expression (12) in the text for $H_0=0.7H_k$.

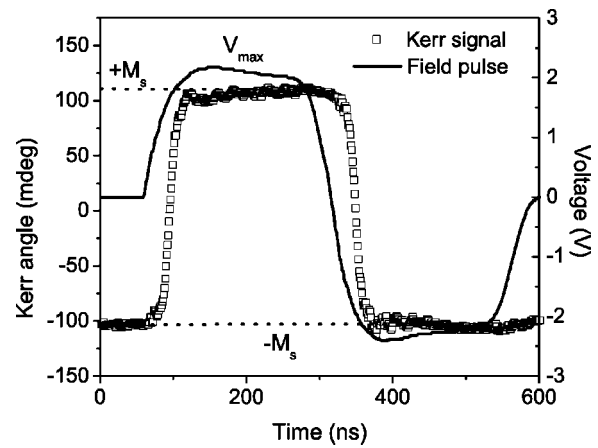


FIG. 3. Temporal Kerr signal acquired at the center of the microcoil for an array of $100 \times 400 \text{ nm}^2$ magnetic dots (squares). The continuous line is an image of the current pulsed in the coil.

since the nuclei can form on smaller defects. In contrast, in the dots, the nucleation rate stays almost independent of v because of the reduced size of the structures. The main contribution to the reversal time is the nucleation one. This last assumption was confirmed experimentally since the coercivity of the dots arrays was found to be almost independent of the dot size over a rather large range of size (400–90 nm). Assuming the existence of only one nucleation center per dot, i.e., one barrier per dot, and neglecting the propagation process, we can use expression (12) to calculate the average coercivity. As discussed previously, the initial nucleation appears on a local defect corresponding to a local reduction of anisotropy or exchange. We describe this reduction by introducing a reduction factor ϵ in γ with $\epsilon < 1$. The other parameters such as the magnetization, the exchange and the anisotropy were determined from other experiments ($A=0.28 \times 10^{-11} \text{ J/m}$, $K_{eff}=2.2 \times 10^5 \text{ J/m}^3$, and $M_S=1.4 \times 10^6 \text{ A/m}$). A good agreement between experi-

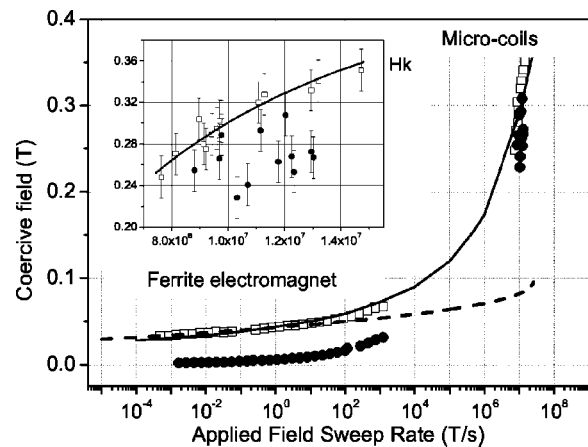


FIG. 4. Evolution of the average dynamical coercive field vs the field sweep rate for the magnetic dots (squares) and for the unpatterned layer (dots) on the entire field sweep range. The continuous line a fit using expression (12) in the text for $\epsilon=0.7$. The dashed line is another fit using the SW-type model (expression (2)) with $E_n=60k_B T$ and $H_n=0.085 \text{ T}$ (see Ref. 16 for the formula).

mental points and the calculated curve is obtained for $\varepsilon=0.7$ and $H_0=\varepsilon H_K$, as shown in Fig. 2.

To reach reversal times closer to τ_0 , microcoils were used to generate the pulsed magnetic field. Figure 3 shows the current pulse sent into the microcoil as well as the magnetic response. The reversal is achieved before the voltage V reaches its maximum value V_{max} . The field rate v is the average slope of the initial ramp, the field strength being calculated via the current. By increasing V_{max} , it is also possible to vary the field rate and thus, to obtain several hysteresis loops corresponding to different v . Figure 4 shows the variation of the dynamical coercivity for the patterned and unpatterned layers over 12 orders of magnitudes of v explored with the ferrite electromagnet and the microcoils. In the fastest dynamical regime, where the reversal is achieved in 20 ns, both dynamical coercive fields are close to the anisotropy field H_K whereas they were quite different at low frequencies [see Figs. 2(a) and 2(b)]. The continuous line in Fig. 4 shows the calculated coercive field using expression (12) for the same ε and H_0 than previously determined. To compare with a SW-type model, we have calculated the coercive field using the barrier form (2) with $\alpha=2$ and we have plotted it in Fig. 4 as well (dashed line, see Ref. 13 for the formula used). It is clear that assuming a power-law dependence of the energy barrier on the applied field does not allow to reproduce the experimental data in the entire field sweep rate range, whereas the droplet model fits them very well. The droplet

model could also be used to model the dynamic reversal of the continuous layer provided the distribution of defects (amplitude and density) and domain wall velocity were known. In particular, this means that the droplet model presented here may be more adapted than the widely used Sharrock model¹⁵ for the interpretation of the dynamic coercivity of recording media over a large range of characteristic field sweep rate.

In conclusion, by investigating the dynamical coercivity of (Pt/Co) multilayers over 12 orders of magnitude, we were able to show that the nucleation process, in perpendicular magnetized layers, follows an activation law proportional to the inverse of the applied field. In addition, it was shown that in arrays of deeply submicronic dots, there is only one nucleation center per dot. When the transition time is close to τ_0 , the coercive fields of the patterned and unpatterned layers are both found to be equal to H_K , which is the field strength required to switch the magnetization by coherent rotation. The evidence of a $1/H$ activation law in perpendicular systems should lead to other criteria for the magnetic stability in perpendicular media since the grain size or the dot size are larger than the domain wall width.

We wish to acknowledge the Région Rhône-Alpes and Institut de Physique de la Matière Condensée for financial support.

*Corresponding author. Electronic address: moritz@cea.fr

¹W. Wernsdorfer, E. Bonet Orozco, K. Hasselbach, A. Benoit, B. Barbara, N. Demoncy, A. Loiseau, H. Pascard, and D. Maily, *Phys. Rev. Lett.* **78**, 1791 (1997).

²D. Atkinson, D. A. Allwood, G. Xiong, M. D Cooke, C. C. Faulkner, and R. P. Cowburn, *Nat. Mater.* **2**(2), 85 (2003).

³H. W. Schumacher, C. Chappert, R. C. Sousa, and P. P. Freitas, *Appl. Phys. Lett.* **83**, 2205 (2003).

⁴E. C. Stoner and E. P. Wohlfarth, *Philos. Trans. R. Soc. London, Ser. A* **240**, 599 (1948).

⁵R. H. Victora, *Phys. Rev. Lett.* **63**, 457 (1989).

⁶P. Bruno, G. Bayreuther, P. Beauvillain, C. Chappert, G. Lugert, and D. Renard, *J. Appl. Phys.* **68**, 5759 (1990); see also G. Bayreuther, P. Bruno, G. Lugert, and C. Turtur, *Phys. Rev. B* **40**, 7399 (1989).

⁷M. P. Sharrock, *J. Appl. Phys.* **76**, 6413 (1994).

⁸B. Raquet, M. D. Ortega, M. Goiran, A. R. Fert, J. P. Redoules, R. Mamy, J. C. Ousset, A. Sdaq, and A. Khmou, *J. Magn. Magn. Mater.* **150**, L5 (1995).

⁹B. Barbara, *J. Magn. Magn. Mater.* **129**, 79 (1994).

¹⁰A. Aharoni and W. Baltensperger, *Phys. Rev. B* **45**, 9842 (1992).

¹¹L. Néel, *Ann. Geophys. (C.N.R.S.)* **5**, 99 (1949).

¹²W. F. Brown, Jr., *Phys. Rev.* **130**, 1677 (1963).

¹³J. Moritz, B. Dieny, J. P. Nozières, S. Landis, A. Lebib, and Y. Chen, *J. Appl. Phys.* **91**, 7314 (2002).

¹⁴M. Bonfim, K. Mackay, S. Pizzini, M. L. Arnou, A. Fontaine, G. Ghiringhelli, S. Pascarelli, and T. Neisius, *J. Appl. Phys.* **87**, 5974 (2000).

¹⁵R. P. Cowburn, D. K. Koltsov, A. O. Adeyeye, M. E. Welland, and D. M. Tricker, *Phys. Rev. Lett.* **83**, 1042 (1999).

¹⁶B. Raquet, R. Mamy, and J. C. Ousset, *Phys. Rev. B* **54**, 4128 (1996).